Analysis of Adaptive Beamforming Techniques for Photonics-based Coherent MIMO Radars

Salvatore Maresca
IEIIT Institute
National Research Council (CNR)
Pisa, Italy
salvatore.maresca@cnr.it

Antonio Malacarne
PNTLab Institute
Nat. Interuniv. Cons. for Telecom. (CNIT)
Pisa, Italy
antonio.malacarne@cnit.it

Malik Muhammad Haris Amir
TeCIP Institute
Sant'Anna School of Advanced Studies (SSSA)
Pisa, Italy
malikmuhammadharis.amir@santannapisa.it

Gaurav Pandey
TeCIP Institute
SSSA
Pisa, Italy
gaurav.pandey@santannapisa.it

Antonella Bogoni
PNTLab Institute
CNIT
Pisa, Italy
antonella.bogoni@cnit.it

Mirco Scaffardi
PNTLab Institute
CNIT
Pisa, Italy
mirco.scaffardi@cnit.it

2023 IEEE International Workshop on Technologies for Defense and Security (TechDefense) | 979-8-3503-1939-2/23/$31.00 ©2023 IEEE | DOI: 10.1109/TechDefense59795.2023.10380917

***Abstract*—In this paper, adaptive beamforming techniques are applied to photonics-based coherent multiple-input multiple-output (MIMO) radars with widely separated antennas for obtaining high target resolution and sidelobe suppression capabilities in the MIMO ambiguity function (MIMO-AF). Among the available MIMO beamforming techniques, *data-independent* and *data-dependent* approaches do exist. In this paper, one estimation technique per family is analyzed (i.e., data-independent, data-dependent without array steering vector errors and data-dependent with array steering vector errors). More specifically, the least-squares estimator, the Capon and the robust Capon beamformers are investigated.**

Key performance indicators (KPIs) are identified for describing the resolution and sidelobe suppression capabilities of the proposed techniques. Simulations are performed to evaluate the KPIs from the MIMO-AF under non-ideal conditions, such as amplitude mismatches among the radar channels and antenna positions affected by random errors. The advantages and disadvantages of the proposed adaptive beamforming techniques are illustrated.

***Index Terms*—Microwave Photonics, Photonics-based Radar, MIMO Radar, Distributed Radar, Coherent MIMO Radar, Adaptive Beamforming, Least-Squares, Capon Beamformer, Robust Capon Beamformer.**

I. Introduction

Since one of the first studies appeared in the late 90′s [1], multistatic radars have started attracting ever-growing attention beyond traditional monostatic systems, thanks to the possibility to observe a target from multiple viewpoints, and to increased robustness against electronic countermeasures. Later, the idea has been better articulated into a more *network-oriented* approach [2], borrowing from the world of wireless communications the concept of multiple-input multiple-output (MIMO) system.

In MIMO radars, it is possible to distinguish between systems with co-located antennas [3] and systems with widely separated antennas [4]. These latter systems employ multiple, spatially distributed transmitters (TXs) and receivers (RXs) driven by one central unit (CU), as depicted in Fig. 1.

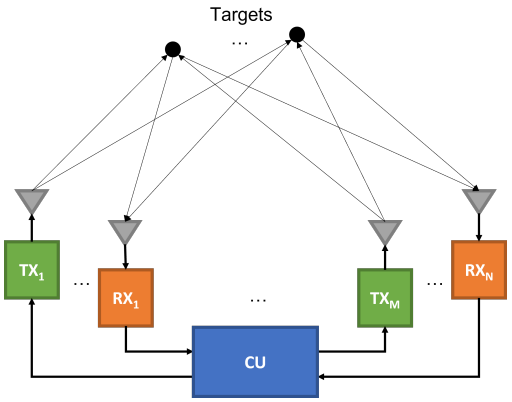

Fig. 1. MIMO radar with widely separated antennas formed by one central unit (CU), acting as the fusion centre, and M transmit (TX) and N receive (RX) remote antennas.

Thus, by employing multiple angles of observation, MIMO radars with widely separated antennas achieve improved target detection performance thanks to radar cross section (RCS) diversity [5], allow the detection of slow-moving targets by exploiting Doppler estimates from multiple directions [6], and can grant high-resolution target localization [7]. Unfortunately, to fully take advantage of these features, high system complexity, fine time and phase synchronization, and large capacity communication links are required.

In this context, microwave photonics (MWP) has emerged as a possible enabling technology for coherent MIMO radars with widely separated antennas [8]–[11]. As a matter of fact, two recent EU-funded projects, i.e., RANGER [12] and ROBORDER [13], have investigated the potentialities of this technology in the field of maritime border security and search-

This work was partially funded within the project COSMOS by the FISR funding scheme, Italian Ministry of University and Research.

and-rescue (SaR) operations.

Starting from the analysis presented in [14] for co-located systems, this paper investigates the possibility to apply adaptive beamforming techniques also to coherent MIMO radars with widely separated antennas for obtaining high-resolution target localization, under ideal and non-ideal conditions (e.g., unknown amplitude mismatch among the channels, antenna positions knowledge affected by errors).

The available adaptive beamforming techniques can be categorized into *data-independent* and *data-dependent* approaches. The least squares (LS) method belongs to the first category [14]. A further categorization can be made of data-dependent beamforming algorithms, whether there are, or not, array steering vector errors [14]. In absence of array steering vector errors, it is possible to mention the Capon [15], the amplitude and phase estimation (APES) [16], the combined Capon and APES (CAPES) [17], as well as the combined Capon and approximate maximum likelihood (CAML) [18] algorithms. In presence of array steering vector errors, the robust Capon beamformer (RCB) [19], [20], and the doubly constrained robust Capon beamformer (DCRCB) [21] can be applied.

In this paper, only one estimation technique per family will be analyzed (i.e., data-independent, data-dependent without array steering vector errors, and data-dependent with array steering vector errors): the LS, the Capon and the RCB estimators. Following the analysis presented in [22], relevant key performance indicators (KPIs) are used for evaluating the effectiveness of the proposed techniques.

The paper is organized as follows. In Section II, the adaptive beamforming techniques for MIMO radar are described, starting from the MIMO signal model. System non-idealities are introduced in Section III, together with mitigation techniques. In Section IV, the proposed beamforming algorithms are analyzed by means of computer simulations. Finally, conclusions and perspectives are provided in Section V.

II. Adaptive Beamforming for MIMO Radar

As described in [4], the standard techniques for MIMO radars are based on non-coherent MIMO processing, where the system works in *search mode*, and coherent MIMO processing, where the system works in *image mode*, with the possibility of obtaining resolution beyond the one granted by the waveform bandwidth. In MIMO radars with co-located antennas, by transmitting independent waveforms via different antennas, the echoes due to targets at different locations result linearly independent of each other. Even more so, in MIMO radars with widely separated antennas, which also exploit geometric diversity, this condition may allow, as in case of co-located systems, the direct application of data-independent and data-dependent adaptive beamforming techniques [14].

A. Signal Model

The received signal matrix can be written as [14]:

$$\mathbf{X} = \mathbf{a}_{RX}(\theta)\,\beta(\theta)\,\mathbf{a}_{TX}^{t}(\theta)\,\mathbf{S} + \mathbf{Z}, \tag{1}$$

where:

- $\mathbf{X} \in \mathbb{C}^{N\times L}$: RX signal matrix;
- M/N: arbitrarily located TX/RX antennas;
- L: number of samples;
- $\mathbf{a}_{RX}(\theta) \in \mathbb{C}^{N\times 1}$: RX antenna steering vector;
- $\mathbf{a}_{TX}(\theta) \in \mathbb{C}^{M\times 1}$: TX antenna steering vector;
- $\mathbf{S} = [\mathbf{s}_1, \ldots, \mathbf{s}_M]^t$: TX signal matrix;
- $\mathbf{s}_m \in \mathbb{C}^{L\times 1}$: generic TX signal at the m-th antenna element, with $m = 1, 2, \ldots, M$;
- $\beta(\theta) \in \mathbb{C}^{1\times 1}$: complex amplitude of the reflected signal from θ, proportional to the RCS of the focal point θ;
- $\mathbf{Z} \in \mathbb{C}^{N\times L}$: residual noise term (e.g., un-modeled noise, interference from targets, jamming).

For conciseness, the dependency of $\mathbf{a}_{RX}(\theta)$ and $\mathbf{a}_{TX}(\theta)$ from θ will be omitted.

B. Adaptive Beamforming Techniques

1) LS Estimator: A simple way to estimate $\beta(\theta)$ in eq. 1 consists of using the LS method [14]:

$$\hat{\beta}_{LS}(\theta) = \frac{\mathbf{a}_{RX}^{H}\mathbf{X}\mathbf{S}^{H}\mathbf{a}_{TX}^{*}}{L\|\mathbf{a}_{RX}\|^2\left[\mathbf{a}_{RX}^{t}\hat{\mathbf{R}}_{\mathbf{SS}}\mathbf{a}_{TX}^{*}\right]}, \tag{2}$$

with $\hat{\mathbf{R}}_{\mathbf{SS}} = \mathbf{S}\mathbf{S}^{H}/L$ and where $(.)^{H}$, $(.)^{*}$ and $(.)^{t}$ denote the conjugate transpose, the complex conjugate and the transpose, respectively, $\|.\|$ denotes the Euclidean norm, and $\hat{\mathbf{R}}_{\mathbf{SS}}$ is the correlation matrix of the waveforms. However, being a data-independent beamforming-type method, the LS method suffers from high sidelobes and low resolution.

2) Capon Estimator: The Capon estimator is a data-dependent approach, consisting of two main steps. The first is the Capon beamforming step [15]. The second is an LS estimation step, which involves a matched filtering procedure. The Capon estimate of $\beta(\theta)$ is given as follows:

$$\hat{\beta}_{Capon}(\theta) = \frac{\mathbf{a}_{RX}^{H}\hat{\mathbf{R}}^{-1}\mathbf{X}\mathbf{S}^{H}\mathbf{a}_{TX}^{*}}{L\left[\mathbf{a}_{RX}^{H}\hat{\mathbf{R}}^{-1}\mathbf{a}_{RX}\right]\left[\mathbf{a}_{TX}^{t}\hat{\mathbf{R}}_{SS}\mathbf{a}_{TX}^{*}\right]}, \tag{3}$$

where $\hat{\mathbf{R}} = \mathbf{X}\mathbf{X}^{H}/L$ is the sample covariance of the observed data samples.

3) RCB Estimator: The previous methods assume that the transmitting and receiving arrays are perfectly calibrated, i.e., $\mathbf{a}_{TX}$ and $\mathbf{a}_{RX}$ are accurately known as functions of θ. The RCB estimator can be successfully applied to a MIMO radar system that suffers from calibration errors [19].

In fact, the RCB algorithm allows $\mathbf{a}_{RX}$ to lie in an uncertainty set. Without loss of generality, we assume that $\mathbf{a}_{RX}$ belongs to the uncertainty sphere $\|\mathbf{a}_{RX} - \bar{\mathbf{a}}_{RX}\|^2 \leq \epsilon$, with both $\bar{\mathbf{a}}_{RX}$, i.e., the nominal receiving array steering vector, and ϵ being given. It is worth noticing that the calibration errors in $\mathbf{a}_{TX}$ will also degrade the accuracy of the estimate of $\beta(\theta)$. However, the LS approach of the Capon beamformer, see eq. 2, is quite robust against calibration errors in $\mathbf{a}_{TX}$. By using the Lagrange multiplier methodology, as described in [19], it is possible to write:

$$\hat{\mathbf{a}}_{RX}(\theta) = \bar{\mathbf{a}}_{RX}(\theta) - \left[\mathbf{I} - \lambda(\theta)\,\hat{\mathbf{R}}\right]^{-1}\bar{\mathbf{a}}_{RX}(\theta), \tag{4}$$

where $\mathbf{I}$ denotes the identity matrix. The Lagrange multiplier $\lambda(\theta)$ is obtained as the solution to the constraint equation [19]:

$$\left\| \left[\mathbf{I} - \lambda(\theta) \hat{\mathbf{R}} \right]^{-1} \bar{\mathbf{a}}_{RX}(\theta) \right\|^2 = \epsilon, \tag{5}$$

Once the Lagrange multiplier $\lambda(\theta)$ has been determined, $\hat{\mathbf{a}}_{RX}(\theta)$ is obtained from eq. 4. To eliminate a scaling ambiguity discussed in [19], it is necessary to scale $\hat{\mathbf{a}}_{RX}(\theta)$ such that $\|\hat{\mathbf{a}}_{RX}(\theta)\|^2 = N$. Replacing $\mathbf{a}_{RX}$ in eq. 3 with $\hat{\mathbf{a}}_{RX}$ yields the RCB estimate of $\beta(\theta)$.

III. System Non-Idealities

The parameter which describes the amplitude mismatch among the radar channels is the standard deviation of the normalized amplitude error (K_A). The parameter which describes the not-perfect knowledge of the sensor positions is the standard deviation of the normalized displacement error (K_D). Both parameters can be calculated as:

$$K_A = \frac{\sigma_A}{A}, K_D = \frac{\sigma_D}{\lambda_{RF}}, \tag{6}$$

where A is the signal amplitude and σ_A is the amplitude variance, and where λ_{RF} is the signal wavelength and σ_D is the sensor displacement standard deviation.

IV. Algorithm Analysis

To understand the effectiveness of the proposed techniques, an extensive analysis of all the estimators is performed under different operational conditions, often diverging from the ideal conditions, aimed at estimating the target locations and the reflected signal amplitudes $\beta(\theta)$. The analysis is conducted comparing the LS, Capon and RCB algorithms through both non-coherent and coherent MIMO processing approaches.

A. Simulations in absence of system non-idealities

In case of no amplitude and no antenna displacement errors, the in-door experimental scenario described in [23] is replicated, with the following system setup parameters:

- $M = 2$ TXs and $N = 4$ RXs over a 3 m baseline;
- Target distance from the baseline center equal to 4 m;
- Frequency $f_{RF} = 10$ GHz, bandwidth $B = 1$ GHz;
- Phase noise due to signal distribution over optical fiber links modelled according to [24].

Results relative to the ambiguity functions are depicted in Fig. 2 for all the proposed estimators. Here, it is possible to highlight the strong similarities between the coherent MIMO processing, see Fig. 2 (b), and the LS, see Fig. 2 (c), processing outputs. As remarked in [4], [14], they both derive from mathematical formulations of the matched filter. Under ideal operative conditions, the Capon and RCB estimators, see Fig. 2 (d,e), show very similar results. Here, in fact, the amount and intensity of sidelobes has significantly diminished, together with a remarkable improvement of the cross-range resolution. The reason behind these improvements should be found in the data-dependent nature of the two algorithms [14], [19].

B. Simulations in presence of system non-idealities

In this analysis, the effects of amplitude and antenna displacement errors are investigated, see Section III. For the simulations, the same system parameters described in Section IV-A are considered, with the exception of the target distance which is now 30 m from the baseline center. Both K_A and K_D parameters vary in the set $\{1/10000, 1/1000, 1/100, 1/10, 1\}$. For each coefficient value, 100 Monte Carlo simulations are run, in which the errors are randomly generated.

The effects of the two types of error are quantitatively evaluated in a separate manner considering the following KPIs: range (ΔR) and cross-range (ΔXR) resolution, root mean square error (RMSE) of the estimated target position, peak-to-maximum sidelobe ratio (PMSR) and peak-to-average sidelobe ratio (PASR), see [22].

According to the analysis presented in [24], the effect of phase noise due to signal distribution over optical fiber links can be neglected for fiber spans shorter than 20 km.

1) Analysis of range and cross-range resolutions: Results of the analysis on ΔR and ΔXR are plotted in Fig. 3 and Fig. 4, respectively. As depicted in Fig. 3, in the ideal case, ΔR is approximately 0.18 m, i.e., very close to the theoretical value of 0.15 m given a signal bandwidth of 1 GHz. All the proposed techniques achieve very similar results, see Fig. 3(a-d). Interestingly, with increasing error, ΔR apparently diminishes. This unexpected result requires further analysis.

In the ideal case, ΔXR is approximately 0.18 m at 30 m range (i.e., angular resolution of $0.35°$) for the coherent MIMO and LS estimator outputs, see Fig. 4(a,b). When the Capon and RCB estimators are used, see Fig. 4(c,d), ΔXR diminishes to 0.06 m at 30 m (i.e., $0.12°$).

Against signal amplitude errors, ΔR and ΔXR worsen for $K_A > 1/10$. These effects are more evident on cross-range resolution when the Capon and RCB estimators are employed, see red curves in Fig. 4(c,d). Against antenna position errors, ΔXR is more affected than ΔR, especially when data-dependent beamformers are used, meaning that these techniques are very sensitive to both types of error.

2) Localization accuracy: Results of the analysis on localization root-mean squared error ($RMSE$) are plotted in Fig. 5. In the case of coherent MIMO and LS estimators, signal amplitude errors have almost no effect on the KPI, see red curves in Fig. 5(a,b), whereas antenna position errors start having effect on it when $K_D > 1/10$, see yellow curves in Fig. 5(a,b). Instead, for the Capon and RCB estimators, $RMSE$ worsens for $K_A > 1/10$ and $K_D > 1/100$, see red and yellow curves in Fig. 5(c,d), respectively.

3) Sidelobe suppression capability: Results of the analysis on $PMSR$ and $PASR$ are plotted in Fig. 6 and Fig. 7, respectively. The values of $PMSR$ is around 2 dB for the coherent MIMO and LS estimators, see Fig. 6(a,b). The effect of signal amplitude and antenna displacement errors is $\leq$ 1 dB. Again, Capon and RCB beamformers, which under ideal conditions grant $PMSR \approx 13$ dB, are very intolerant to both amplitude and antenna displacement errors, see Fig. 6(c,d). In fact, when K_A or K_D are large, the two

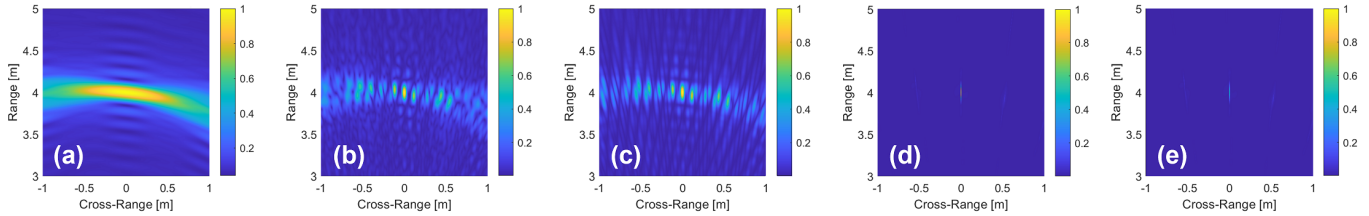

Fig. 2. Analysis of the adaptive beamforming algorithms in the absence of system non-idealities and one target at 4 m distance from the baseline: (a) non-coherent MIMO output, (b) coherent MIMO output, (c) LS estimator, (d) Capon estimator, (e) RCB estimator.

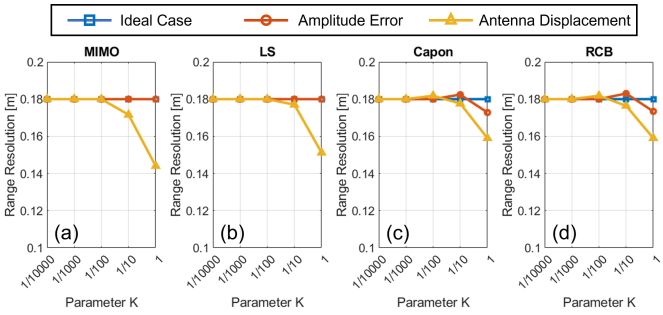

Fig. 3. Analysis of range resolution (ΔR) at the varying of K_A/K_D parameters: (a) Coherent MIMO, (b) LS estimate, (c) Capon beamformer, (d) RCB estimate.

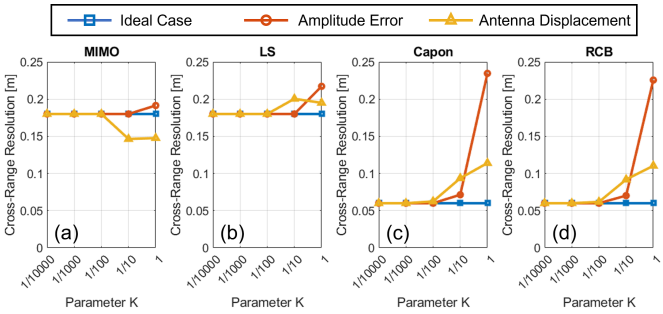

Fig. 4. Analysis of cross-range resolution (ΔXR) at the varying of K_A/K_D parameters: (a) Coherent MIMO, (b) LS estimate, (c) Capon beamformer, (d) RCB estimate.

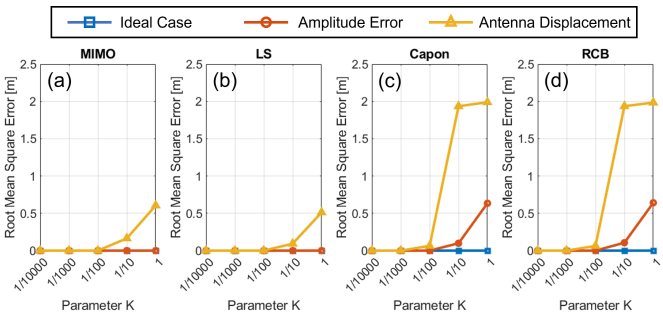

Fig. 5. Analysis of root mean square error ($RMSE$) at the varying of K_A/K_D parameters: (a) Coherent MIMO, (b) LS estimate, (c) Capon beamformer, (d) RCB estimate.

data-dependent estimators almost reach the performance of the coherent MIMO and LS estimators.

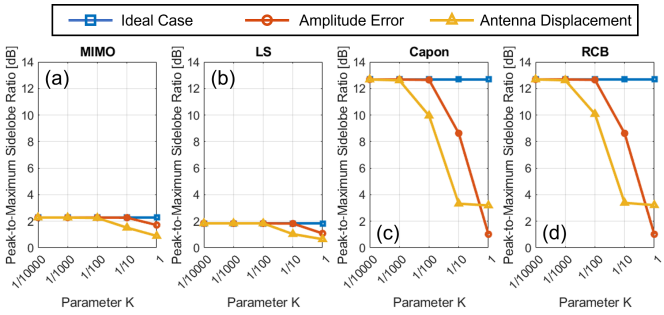

Fig. 6. Analysis of peak-to-maximum sidelobe ratio ($PMSR$) at the varying of K_A/K_D parameters: (a) Coherent MIMO, (b) LS estimate, (c) Capon beamformer, (d) RCB estimate.

Similar comments can be made out of the analysis of $PASR$ in Fig. 7. The coherent MIMO and LS estimators grant almost 20 dB (18 dB of the LS), even in the presence of signal amplitude and antenna displacement errors, see Fig. 7(a,b). The Capon and RCB beamformers achieve around 34 dB in the case of ideal conditions, see Fig. 7(c,d). However, their performance worsen when K_A or K_D are greater than $1/100$, leading to $PASR$ values similar to those achieved by coherent MIMO and LS estimators.

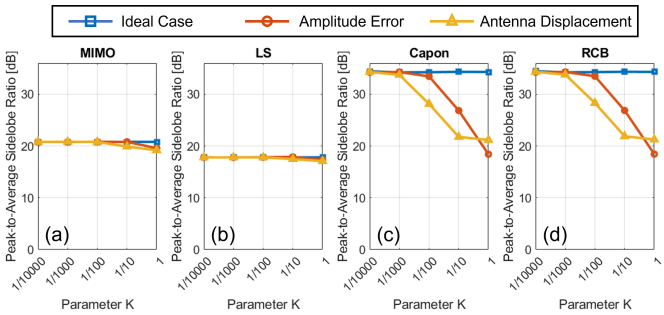

Fig. 7. Analysis of peak-to-average sidelobe ratio ($PASR$) at the varying of K_A/K_D parameters: (a) Coherent MIMO, (b) LS estimate, (c) Capon beamformer, (d) RCB estimate.

V. Conclusion

In this paper, adaptive beamforming techniques have been applied to photonics-based coherent MIMO radars with widely separated antennas. Non-ideal operative conditions have been

considered, such as amplitude mismatch among the radar channels, antenna positions knowledge affected by errors.

Both data-independent and data-dependent MIMO beamforming techniques have been considered. More specifically, the LS, the Capon and the RCB estimators have been presented and analyzed. Simulations have been performed to analyze the effectiveness of the proposed methods in close-to-reality operative conditions.

Among all the analyzed algorithms, Capon and RCB clearly perform better than LS and coherent MIMO outputs, in terms of cross-range resolution, which has improved by a factor of 3, and in terms of PMSR and PASR, which have improved by more than 10 dB each. Conversely, the data-dependent nature of Capon and RCB estimators is also the reason why they are much more sensitive to non-idealities than coherent MIMO and LS estimators, leading to even worse performance under certain particularly detrimental conditions.

For this reason, it is necessary to implement post-processing techniques for mitigating, not only array calibration errors, but also antenna positioning errors, as well as synchronization errors among the radar channels if the fiber span lengths are in the order of tens of kilometers. These issues are currently under further investigation.

REFERENCES

[1] V. S. Chernyak, Fundamentals of Multisite Radar Systems, Routledge, 1998.

[2] E. Fishler, *et al.*, "MIMO radar: An idea whose time has come," *IEEE Radar Conf.*, pp. 71–78, 2004.

[3] J. Li, P. Stoica, "MIMO Radar with Colocated Antennas," *IEEE Sig. Proc. Mag.*, vol. 24, no. 5, pp. 106-114, Sept. 2007.

[4] A. M. Haimovich, *et al.*, "MIMO Radar with Widely Separated Antennas," *IEEE Sig. Proc. Mag.*, vol. 25, no. 1, pp. 116-129, 2008.

[5] E. Fishler, *et al.*, "Spatial diversity in radars—Models and detection performance", *IEEE Trans. Signal Process.*, vol. 54, pp. 823-838, 2006.

[6] N. Lehmann, *et al.*, "MIMO-radar application to moving target detection in homogenous clutter", Adaptive Sensor Array Processing Workshop at MIT Lincoln Laboratory, 2006.

[7] N. H. Lehmann, *et al.*, "High resolution capabilities of MIMO radar", Proc. 40th Asilomar Conf. Signals Systems and Computers, 2006.

[8] J. Capmany, D. Novak, "Microwave photonics combines two worlds", *Nature Photonics*, vol. 1, pp. 319-330, 2007.

[9] J. McKinney, "Photonics illuminates the future of radar", *Nature*, vol. 507, pp. 310-312, 2014.

[10] A. Bogoni, P. Ghelfi and F. Laghezza, Photonics for Radar Networks and Electronic Warfare Systems, London:IET SciTech Pub., 2019.

[11] G. Serafino, *et al.*, "Microwave Photonics for Remote Sensing: From Basic Concepts to High-Level Functionalities", *IEEE J. of Light. Tech.*, vol. 38, no. 19, pp. 5339-5355, 2020.

[12] RANGER: RAdars for loNG distance maritime surveillancE and SaR opeRations, https://cordis.europa.eu/project/id/700478.

[13] ROBORDER: autonomous swarm of heterogeneous RObots for BORDER surveillance, https://cordis.europa.eu/project/id/740593.

[14] L. Xu, *et al.*, "Target detection and parameter estimation for MIMO radar systems," *IEEE Trans. Aerosp. Electron. Syst.*, vol. 44, no. 3, pp. 927-939, 2008.

[15] J. Capon, "High resolution frequency-wavenumber spectrum analysis," *Proc. IEEE*, vol. 57, pp. 1408—1418, 1969.

[16] J. Li, and P. Stoica, "An adaptive filtering approach to spectral estimation and SAR imaging", *IEEE Transactions on Signal Processing*, vol. 44, pp. 1469-1484, June 1996.

[17] A. Jakobsson and P. Stoica, "Combining Capon and APES for estimation of spectral lines", *Circuits Systems and Signal Processing*, vol. 19, no. 2, pp. 159-169, 2000.

[18] L. Xu, P. Stoica and J. Li, "A diagonal growth curve model and some signal processing applications", *IEEE Transactions on Signal Processing*, vol. 54, pp. 3363-3371, Sept. 2006.

[19] J. Li, *et al.*, "On robust Capon beamforming and diagonal loading," *IEEE Trans. Signal Process.*, vol. 51, pp. 1702—1715, 2003.

[20] P. Stoica, Z. Wang and J. Li, "Robust Capon beamforming", *IEEE Signal Processing Letters*, vol. 10, pp. 172-175, June 2003.

[21] J. Li, P. Stoica and Z. Wang, "Doubly constrained robust Capon beamformer", *IEEE Transactions on Signal Processing*, vol. 52, pp. 2407-2423, Sept. 2004.

[22] G. Serafino, *et al.*, "Key Performance Indicators for System Analysis of MIMO Radars with Widely Separated Antennas," 19th European Radar Conference (EuRAD), Milan, Italy, 2022.

[23] A. Malacarne, *et al.*, "Coherent Dual-Band Radar-Over-Fiber Network With VCSEL-Based Signal Distribution," *IEEE J. Light. Technol.*, vol. 38, no. 22, pp. 6257-6264, 2020.

[24] A. Malacarne, *et al.*, "Robustness of Photonics-based Coherent Multi-Band MIMO Radar to Fiber-based Signal Distribution," 20th European Radar Conference (EuRAD), Berlin, Germany, 2023 (accepted).